

Spin- $\frac{5}{2}$ resonance effects in a coupled channel nucleon resonance analysis *

V. Shklyar,[†] G. Penner, and U. Mosel

Institut für Theoretische Physik, Universität Giessen, D-35392 Giessen, Germany

Spin- $\frac{5}{2}$ resonance contributions in pion-nucleon scattering are investigated within the coupled channel K -matrix approach for c.m. energies up to $\sqrt{s} = 2$ GeV. All previously studied πN , $2\pi N$, ηN , $K\Lambda$, $K\Sigma$, and ωN final states are included. We find a significant improvement of χ^2 in almost all channels by inclusion of the spin- $\frac{5}{2}$ states. The obtained coupling parameters are discussed.

PACS numbers: 11.80.-m, 13.75.Gx, 14.20.Gk, 13.30.Gk

I. INTRODUCTION

The extraction of baryon-resonance properties is one of the important tasks of modern hadron physics. Great efforts have been made in the past to obtain this information from the analysis of pion- and photon-induced reaction data. The precise knowledge of these properties is an important step towards understanding the hadron structure and finally the strong interactions. However, until now there are states whose properties are not settled or whose existence is rather controversial. At the same time even some resonances with four-star status have their parameters in a wide range as extracted from different analyses [1]. This complicates the comparison of the extracted parameters with theoretical model predictions. On the other hand, some quark models (see [2] and Refs. therein) predict that the baryon resonance spectrum may be richer than discovered so far. This is a problem of 'missing' nucleon resonances. One assumes that these states are weakly coupled to pion channels and are consequently not clearly seen in πN and $2\pi N$ reactions from which experimental data are most often used for baryon-resonance analyses. To solve these problems additional final states must be taken into account. Ideally a comprehensive analysis should include all open channels and take all experimental reaction data into account.

A large number of models were suggested to obtain resonance properties by using the experimental data from hadronic reactions only ([3, 4, 5]; see also [1] for references). All these analyses apply different unitarization methods for the T -matrix and deal with various data sets. In [3] the authors use only the πN data where inelastic reactions are approximated by a "generic" $\pi\Delta$ channel. The analysis of Manley and Saleski [4] uses both πN and $2\pi N$ production data whereas the most recent studies of Vrana et al. [5] include $\pi N \rightarrow \eta N$ cross sections data in addition to the last two ones. To incorporate other possible final states a unitary coupled channel model (Giessen model) has been developed which includes γN , πN , $2\pi N$, ηN , $K\Lambda$ final states and deals with all available experimental data on pion- and photon-induced reactions [6, 7]. Most recent extensions of this model include $K\Sigma$ and ωN final states [8, 9] as well, which allows for the simultaneous analysis of all hadronic and photoproduction data up to $\sqrt{s} = 2$ GeV. A shortcoming of this study is the missing of higher spin resonances with spin $J > \frac{3}{2}$. A successful description of data for all final states has nevertheless been achieved in [8] and at first sight there is not much evidence that higher-spin resonances can give significant contributions to the final states studied. However, for a comprehensive analysis of baryon spectra the contributions from higher spin resonances must be included as well. It is known as well, that spin- $\frac{5}{2}$ resonances have large electromagnetic couplings [1] and have to be included into photon-induced reaction analyses. To improve the situation we extend our model by including resonance states with spin $\frac{5}{2}$. In the present paper we report our first results on the pion-induced reactions studied; the simultaneous analysis of pion- and photon-induced reactions will be presented in a subsequent paper.

As a first step we keep all ingredients of our last study taking into account the πN , $2\pi N$, ηN , $K\Lambda$, $K\Sigma$, and ωN final states and include in addition the spin- $\frac{5}{2}$ resonances that were absent in [6, 7, 8, 9]. We do not look for additional open channels but instead check the evidence for additional resonance states which have a one or two stars status rated by [1]. We start in Sec. II with a description of the formalism concentrating mainly on the spin- $\frac{5}{2}$ couplings; the complete discussion of our model including all other couplings can be found in [8, 9, 10]. Sec. III is devoted to details of calculations. In Secs. IV and V we discuss the results of our calculations in comparison with the previous studies [8]. We present the extracted resonance masses and partial decay widths and finish with a summary.

* Supported by DFG and GSI Darmstadt

[†] Electronic address: shklyar@theo.physik.uni-giessen.de

II. THE GIJESSEN MODEL

We solve the Bethe-Salpeter coupled-channel equation in the K -matrix approximation to extract scattering amplitudes for the final states under consideration. In order to decouple the equations we perform partial-wave decomposition of the T matrix into good total spin J , isospin I , and parity $P = (-1)^{J \pm \frac{1}{2}}$. Then the partial-wave amplitudes can be expressed in terms of an interaction potential \mathcal{K} via the matrix equation

$$\mathcal{T}^{I,J\pm} = \begin{bmatrix} \mathcal{K}^{I,J\pm} \\ 1 - i\mathcal{K}^{I,J\pm} \end{bmatrix}, \quad (1)$$

where each element of the matrices $\mathcal{T}_{fi}^{I,J\pm}$ and $\mathcal{K}_{fi}^{I,J\pm}$ corresponds to a given initial and final state ($i, f = \pi N, 2\pi N, \eta N, K\Lambda, K\Sigma, \omega N$). The interaction potential is approximated by tree-level Feynman diagrams which in turn are obtained from effective Lagrangians [8, 10]. The \mathcal{T} -matrix (1) fulfills unitarity as long as the \mathcal{K} matrix is hermitian.

The Lagrangian for the spin- $\frac{5}{2}$ resonance decay to a final baryon B and a (pseudo)scalar meson φ is chosen in the form

$$\mathcal{L}_{\varphi BR}^{\frac{5}{2}} = \frac{g_{\varphi BR}}{m_\pi^2} \bar{u}_R^{\mu\nu} \Theta_{\nu\lambda}(a) \Gamma_S u_B \partial_\mu \partial^\lambda \varphi + h.c. \quad (2)$$

with the matrix $\Gamma_S = \mathbb{1}$ if resonance and final meson have identical parity and $\Gamma_s = i\gamma_5$ otherwise. The free spin- $\frac{5}{2}$ Rarita-Schwinger symmetric field $u_R^{\mu\nu}$ obeys the Dirac equation and satisfies the conditions $\gamma_\mu u_R^{\mu\nu} = \partial_\mu u_R^{\mu\nu} = g_{\mu\nu} u_R^{\mu\nu} = 0$ [11].

The off-shell projector $\Theta_{\mu\nu}(a)$ is defined by

$$\Theta_{\mu\nu}(a) = g_{\mu\nu} - a\gamma_\mu\gamma_\nu, \quad (3)$$

where a is the off-shell parameter. In general the interaction Lagrangian (2) can have two off-shell projectors matched with both vector indices of the resonance field tensor. However, as we will see later, a good description of the experimental data can be achieved already with a single parameter a keeping the second one equal to zero. Thus we have found no necessity for additional parameters and to keep our model as simple as possible we use only one off-shell projector in (2).

The widths of the hadronic resonance decays as extracted from the Lagrangian (2) are

$$\Gamma_\pm(R_{\frac{5}{2}} \rightarrow \varphi B) = I \frac{g_{\varphi BR}^2}{30\pi m_\pi^4} k_\varphi^5 \frac{E_B \mp m_B}{\sqrt{s}}. \quad (4)$$

The upper sign corresponds to the decay of the resonance into a meson with the identical parity and vice versa. I is the isospin factor and k_φ , E_B , and m_B are the meson momentum, energy and mass of the final baryon, respectively.

The coupling of the spin- $\frac{5}{2}$ resonances to the ωN final state is chosen to be

$$\mathcal{L}_{\omega N}^{\frac{5}{2}} = \bar{u}_R^{\mu\lambda} \Gamma_V \left(\frac{g_1}{4m_N^2} \gamma^\xi + i \frac{g_2}{8m_N^3} \partial_N^\xi + i \frac{g_3}{8m_N^3} \partial_\omega^\xi \right) (\partial_\xi^\omega g_{\mu\nu} - \partial_\mu^\omega g_{\xi\nu}) u_N \partial_\lambda^\omega \omega^\nu + h.c., \quad (5)$$

where the matrix Γ_V is $\mathbb{1}$ ($i\gamma_5$) for positive (negative) resonance parity and ∂_N^μ (∂_μ^ω) denotes the partial derivative of the nucleon and the ω -meson fields, respectively. The above Lagrangian is constructed in the same manner as the one for spin- $\frac{3}{2}$ in [8]. Similar couplings were also used to describe electromagnetic processes [12, 13, 14, 15]. Since the different parts of (5) contribute at different kinematical conditions we keep all three couplings as free parameters and vary them during the fit. As stressed in [8] the couplings in (5) can not be reliably derived from hadronic data only; photoproduction data are required as an additional constraint to fix the constants. Therefore, in the present study we do not try to fix all ωN couplings but look for the total ωN flux contribution for each resonance state. To save calculation time and for the sake of simplicity, we also do not introduce any off-shell parameters at the ω -meson couplings (5); indeed we found no strong contribution from spin- $\frac{5}{2}$ waves to the ω -production channel. The couplings (5) lead to the helicity-decay amplitudes

$$\begin{aligned} A_{\frac{3}{2}}^{\omega N} &= \frac{\sqrt{E_N \pm m_N}}{\sqrt{5m_N}} \frac{k_\omega}{4m_N^2} \left(-g_1(m_N \mp m_R) + g_2 \frac{(m_R E_N - m_N^2)}{2m_N} + g_3 \frac{m_\omega^2}{2m_N^2} \right), \\ A_{\frac{1}{2}}^{\omega N} &= \frac{\sqrt{E_N \pm m_N}}{\sqrt{10m_N}} \frac{k_\omega}{4m_N^2} \left(g_1(m_N \pm (m_R - 2E_N)) + g_2 \frac{(m_R E_N - m_N^2)}{2m_N} + g_3 \frac{m_\omega^2}{2m_N^2} \right), \\ A_0^{\omega N} &= \frac{\sqrt{(E_N \pm m_N)}}{\sqrt{5m_N}} \frac{k_\omega m_\omega}{4m_N^2} \left(g_1 \pm g_2 \frac{E_N}{2m_N} \pm g_3 \frac{(m_R - E_N)}{2m_N} \right), \end{aligned} \quad (6)$$

with upper (lower) signs corresponding to positive (negative) resonance parity. The lower indices stand for the helicity λ of the final ωN state $\lambda = \lambda_V - \lambda_N$ where we use an abbreviation as follows: $\lambda = 0 : 0 + \frac{1}{2}, \frac{1}{2} : 1 - \frac{1}{2}, \frac{3}{2} : 1 + \frac{1}{2}$. The resonance ωN decay width $\Gamma^{\omega N}$ is written as the sum over the three helicity amplitudes given above:

$$\Gamma^{\omega N} = \frac{2}{(2J+1)} \frac{k_\omega m_N}{2\pi m_R} \sum_{\lambda=0}^{3/2} |A_\lambda^{\omega N}|^2, \quad (7)$$

where $J = \frac{5}{2}$ for the spin- $\frac{5}{2}$ resonance decay.

For practical calculations we adopt the spin- $\frac{5}{2}$ projector in the form

$$\begin{aligned} P_{\frac{5}{2}}^{\mu\nu,\rho\sigma}(q) &= \frac{1}{2}(T^{\mu\rho}T^{\nu\sigma} + T^{\mu\sigma}T^{\nu\rho}) - \frac{1}{5}2T^{\mu\nu}T^{\rho\sigma} \\ &+ \frac{1}{10}(T^{\mu\lambda}\gamma_\lambda\gamma_\delta T^{\delta\rho}T^{\nu\sigma} + T^{\nu\lambda}\gamma_\lambda\gamma_\delta T^{\delta\sigma}T^{\mu\rho} + T^{\mu\lambda}\gamma_\lambda\gamma_\delta T^{\delta\sigma}T^{\nu\rho} + T^{\nu\lambda}\gamma_\lambda\gamma_\delta T^{\delta\rho}T^{\mu\sigma}), \end{aligned} \quad (8)$$

with

$$T^{\mu\nu} = -g^{\mu\nu} + \frac{q^\mu q^\nu}{m_R^2}, \quad (9)$$

which has also been used in an analysis of $K\Lambda$ photoproduction [13]. As is well known the description of particles with spin $J > \frac{1}{2}$ leads to a number of different propagators which have non-zero off-shell lower-spin components. To control these components the off-shell projectors (3) are usually introduced. There were attempts to fix the off-shell parameters and remove the spin- $\frac{1}{2}$ contribution in the case of spin- $\frac{3}{2}$ particles [16]. However, it has been shown [17] that these contributions cannot be suppressed for any value of a . To overcome this problem Pascalutsa suggested gauge invariance as an additional constraint to fix the interaction Lagrangians for higher spins and remove the lower-spin components [18]. Constructing the spin- $\frac{3}{2}$ interaction for a Rarita-Schwinger field $u_{\frac{3}{2}}^\mu$ by only allowing couplings to the gauge-invariant field tensor $U_{\frac{3}{2}}^{\mu\nu} = \partial^\mu u_{\frac{3}{2}}^\nu - \partial^\nu u_{\frac{3}{2}}^\mu$ Pascalutsa derived an interaction which (for example) for the $\pi N \Delta$ coupling is

$$\mathcal{L}_{\pi N \Delta} = f_\pi \bar{u}_N \gamma_5 \gamma_\mu \tilde{U}^{\mu\nu} \partial_\nu \varphi + h.c. \quad (10)$$

where $\tilde{U}^{\mu\nu}$ is the tensor dual to $U^{\mu\nu}$: $\tilde{U}^{\mu\nu} = \varepsilon^{\mu\nu\lambda\rho} U_{\lambda\rho}$ and $\varepsilon^{\mu\nu\lambda\rho}$ is the Levi-Civita tensor. The same arguments can also be applied to spin- $\frac{5}{2}$ particles. In this case the amplitude of meson-baryon scattering can be obtained from the conventional amplitude by the replacement

$$\Gamma_{\mu\nu}(p', k') \frac{P_{\frac{5}{2}}^{\mu\nu,\rho\sigma}(q)}{\not{q} - m_R} \Gamma_{\rho\sigma}(p, k) \rightarrow \Gamma_{\mu\nu}(p', k') \frac{\mathcal{P}_{\frac{5}{2}}^{\mu\nu,\rho\sigma}(q)}{\not{q} - m_R} \Gamma_{\rho\sigma}(p, k) \frac{q^4}{m_R^4}, \quad (11)$$

where $\Gamma_{\rho\sigma}(p, k)$ are vertex functions that follow from (2) and (5) by applying Feynman rules and the projector $\mathcal{P}_{\frac{5}{2}}^{\mu\nu,\rho\sigma}(q)$ is obtained from (8, 9) by the replacement $q^\mu q^\nu / m_R^2 \rightarrow q^\mu q^\nu / q^2$. This procedure is similar to that which has been used in the spin- $\frac{3}{2}$ case [18]. As can be clearly seen, the conventional and the Pascalutsa descriptions give the same results for on-shell particles. It has been shown for the spin- $\frac{3}{2}$ case [19], that both prescriptions are equivalent in the effective Lagrangian approach as long as additional contact interactions are taken into account when the Pascalutsa couplings are used. The differences between these descriptions have been discussed in [8, 20, 21] and here we perform calculations by using both approaches.

In order to take into account the internal structure of mesons and baryons each vertex is dressed by a corresponding formfactor:

$$F_p(q^2, m^2) = \frac{\Lambda^4}{\Lambda^4 + (q^2 - m^2)^2}. \quad (12)$$

Here q is the four momentum of the intermediate particle and Λ is a cutoff parameter. In [8] it has been shown that the formfactor (12) gives systematically better results as compared to other ones, therefore we do not use any other forms for $F(q^2)$. The cutoffs Λ in (12) are treated as free parameters and allowed to be varied during the calculation. However we demand the same cutoffs in all channels for a given resonance spin J : $\Lambda_{\pi N}^J = \Lambda_{\pi\pi N}^J = \Lambda_{\eta N}^J = \dots$ etc., ($J = \frac{1}{2}, \frac{3}{2}, \frac{5}{2}$). This greatly reduces the number of free parameters; i.e. for all spin- $\frac{5}{2}$ resonances there is only one cutoff $\Lambda_{\frac{5}{2}}$ for all decay channels.

Fit	Total π	$\chi^2_{\pi\pi}$	$\chi^2_{\pi 2\pi}$	$\chi^2_{\pi\eta}$	$\chi^2_{\pi\Lambda}$	$\chi^2_{\pi\Sigma}$	$\chi^2_{\pi\omega}$
C-p- $\pi+$ ($\frac{5}{2}$)	2.60	2.60	7.63	1.37	2.14	1.83	1.23
C-p- $\pi+$	2.66	3.00	6.93	1.85	2.19	1.97	1.24
P-p- $\pi+$ ($\frac{5}{2}$)	3.65	3.80	10.06	1.75	2.54	2.93	1.83
P-p- $\pi+$	3.53	3.72	9.62	2.47	2.69	2.92	2.17
C-p- $\pi+$ ($\frac{5}{2}$) [*]	2.46	2.70	7.11	1.37	2.14	1.83	1.23
P-p- $\pi+$ ($\frac{5}{2}$) [*]	3.37	3.72	9.22	1.75	2.54	2.93	1.83

TABLE I: χ^2 of the different fits. The first and third lines are the new best fit results including the spin- $\frac{5}{2}$ resonances. The second and fourth lines correspond to results from our previous study [8]. ^{*}: χ^2 is calculated neglecting experimental spin- $\frac{5}{2}$ partial wave data in πN and $2\pi N$ channels. In all cases the D_{35} data have not been taken into account (see text).

To take into account contributions of the $2\pi N$ channel in our calculations we use the inelastic partial-wave cross section $\sigma_{2\pi N}^{JI}$ data extracted in [22]. To this end the inelastic $2\pi N$ channel is parameterized by an effective ζN channel where ζ is an effective isovector meson with mass $m_\zeta = 2m_\pi$. Thus the ζN is considered as a sum of different ($\pi\Delta$, ρN , etc.) contributions to the total partial-wave $2\pi N$ flux. We allow only resonance ζN -couplings since each background diagram would introduce a meaningless coupling parameter. Despite this approximation the studies [6, 7, 8, 24] have achieved a good description of the total partial wave cross sections [22] and we proceed in our calculations by using the above prescription. For the $R \rightarrow \zeta N$ interaction the same Lagrangians are used as for the $R \rightarrow \pi N$ couplings taking into account the positive parity of the ζ meson.

III. DETAILS OF CALCULATIONS

In our previous work [8] a good description of all hadronic experimental data was achieved. Hence the best hadronic fit results from [8] for the conventional (C-p- $\pi+$) and the Pascalutsa (P-p- $\pi+$) prescriptions are used as starting points in our extended calculations. We apply the same database as in [8] with additional elastic πN data for the spin- $\frac{5}{2}$ partial wave amplitudes taken from the VPI group analysis [25]. For the $2\pi N$ channel we use the spin- $\frac{5}{2}$ partial wave cross sections derived in [22]. Due to the lack of data for higher energies we confine ourselves to the energy region $m_\pi + m_N \leq \sqrt{s} \leq 2$ GeV.

A complete discussion of the fitting procedure can be found in [10]. Here we briefly give the main features of the calculations. During the fit a χ^2 minimization was performed, where χ^2 is defined as

$$\chi^2 = \frac{1}{N} \sum_{n=1}^N \left(\frac{x_c^n - x_e^n}{\Delta x_e^n} \right)^2. \quad (13)$$

Here, N is the total number of datapoints, x_c^n and x_e^n are calculated and experimental values and Δx_e^n is the experimental uncertainty of x_e^n . To reduce the number of free parameters the πN and $2\pi N$ subset of the spin- $\frac{5}{2}$ resonance parameters was varied first to find a satisfying description of the πN and $2\pi N$ data keeping all resonance and background couplings from C-p- $\pi+$ and P-p- $\pi+$ fixed. Since the Pascalutsa coupling is free of any lower-spin off-shell contributions the inclusion of additional spin- $\frac{5}{2}$ resonances does not lead to any modification of the πN and $2\pi N$ lower partial-waves description. On the other hand the conventional couplings give rise to the lower πN and $2\pi N$ partial waves and also modify ηN , $K\Sigma$, $K\Lambda$ and ωN amplitudes due to rescattering effects even for zero couplings in these channels. Therefore, the simultaneous variation of the spin- $\frac{3}{2}$ and - $\frac{5}{2}$ off-shell parameters is also needed.

After a preliminary fitting of the spin- $\frac{5}{2}$ -resonance masses and πN and $2\pi N$ parameters we carry out an overall fit for all non- and resonance couplings in comparison with the available experimental hadronic data. To minimize the number of free parameters we vary only the two coupling constants g_1 , g_2 in the Lagrangian (5). As we will see later, in Sec. IV, a successful description of ω -meson data can be achieved by using these two couplings only.

The resulting χ^2 of our best overall hadronic fits are given in Table I in comparison with our previous results (last two lines). Here we keep the notation of [8]: C-p- $\pi+$ ($\frac{5}{2}$) and P-p- $\pi+$ ($\frac{5}{2}$) are the best new fit results for the conventional and the Pascalutsa coupling calculations. The third and fourth lines show the χ^2 from the previous study. We find a problem with the description of the D_{35} partial wave so the resulting $\chi^2_{\pi\pi}$ turns out to be very large (see the discussion in the next section). Hence $\chi^2_{\pi\pi}$ values given in Table I are calculated by neglecting the πN datapoints for the D_{35} partial wave.

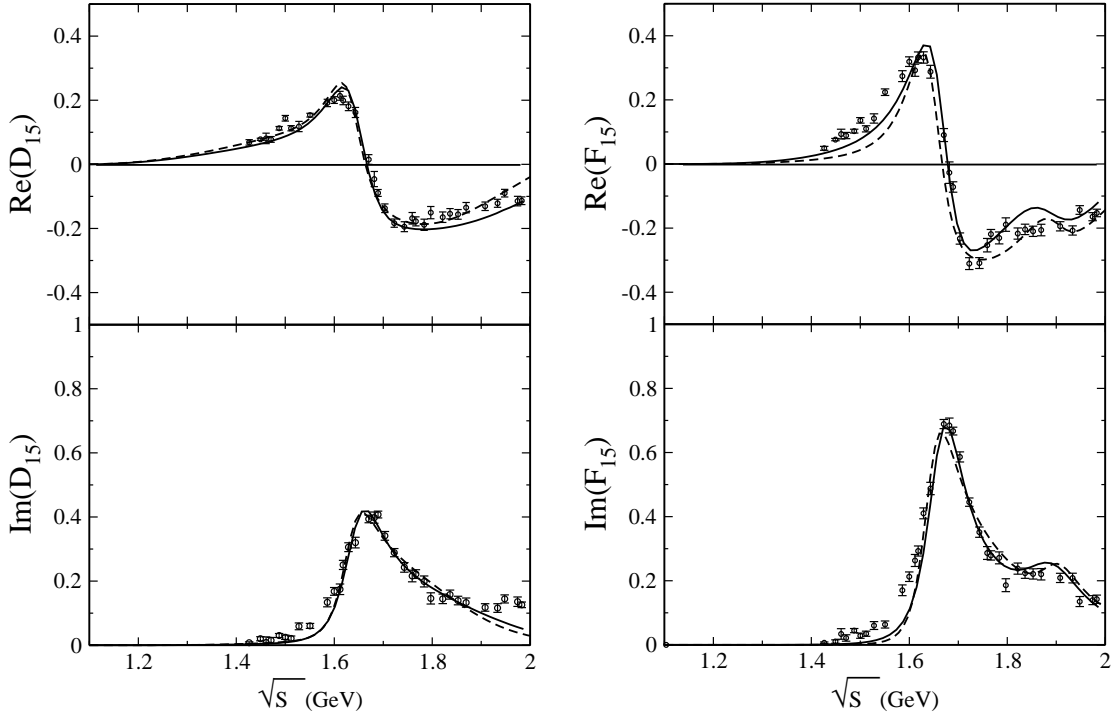


FIG. 1: The elastic $\pi N \rightarrow \pi N$ scattering amplitudes for the spin- $\frac{5}{2}$ partial waves. The solid (dashed) line corresponds to calculation C-p- $\pi + (\frac{5}{2})$ (P-p- $\pi + (\frac{5}{2})$). The data are taken from [25].

One sees from Table I that the inclusion of the spin- $\frac{5}{2}$ resonances leads to an improvement of χ^2 in almost all channels for calculations using the conventional spin- $\frac{5}{2}$ couplings. The only exception is the $2\pi N$ channel where the increase in $\chi^2_{\pi 2\pi}$ is mainly related to the description of the D_{15} and F_{15} partial waves (see next section). Calculations using the Pascalutsa prescription lead to a χ^2 at almost the same level of quality as for our previous results [8]. The obtained new $\chi^2_{\pi\pi}$ and $\chi^2_{\pi 2\pi}$ are calculated using experimental data from all πN and $2\pi N$ partial waves up to spin- $\frac{5}{2}$. For a more reliable comparison with previous results, we have calculated $\chi^2_{\pi\pi}$ and $\chi^2_{\pi 2\pi}$ when only the spin- $\frac{1}{2}$ and $-\frac{3}{2}$ partial wave data were taken into account in (13). The obtained values for the conventional and the Pascalutsa coupling calculations (last two lines in Table I) show that the inclusion of spin- $\frac{5}{2}$ resonances improves the description of the experimental data.

IV. RESULTS AND DISCUSSION

In this section we discuss the results of our calculations for the spin- $\frac{5}{2}$ waves. We stress that the πN partial wave inelasticities are not fitted but obtained as a sum of the individual contributions from all open channels. The $D_{15}(1675)$, $F_{15}(1680)$, and $F_{35}(1905)$ resonances were included in our calculations. We have also found evidence for a second F_{15} state around 1.98 GeV which is rated two-star by [1]. The results for the elastic $\pi N \rightarrow \pi N$ amplitudes and $\pi N \rightarrow 2\pi N$ partial-wave cross sections are shown in Figs. 1 - 3

The πN and $2\pi N$ channels are found to be the dominant decay modes for all four states. In the following each spin- $\frac{5}{2}$ wave is discussed separately.

D_{15} . The elastic VPI data show a single resonant peak which corresponds to the well established $D_{15}(1675)$ state. We find a good description of the elastic amplitude in both the C-p- $\pi + (\frac{5}{2})$ and the P-p- $\pi + (\frac{5}{2})$ calculations.

The $2\pi N$ data [22] are systematically below the total inelasticity of the VPI group [25]. This can be an indication that apart from $2\pi N$ there are additional contributions from other inelastic channels. However, in the analysis of Manley and Saleski [4] as well as in the most recent study of Vrana et al. [5] the total inelasticity in the D_{15} wave is entirely explained by the resonance decay to the $\pi\Delta$ channel. We also find no significant contributions from the ηN , $K\Lambda$, $K\Sigma$, and ωN channels to the total πN inelasticity in the present hadronic calculations. The calculated $2\pi N$ cross sections are found to be substantially above the data from [22] in all fits. Indeed, the difference between

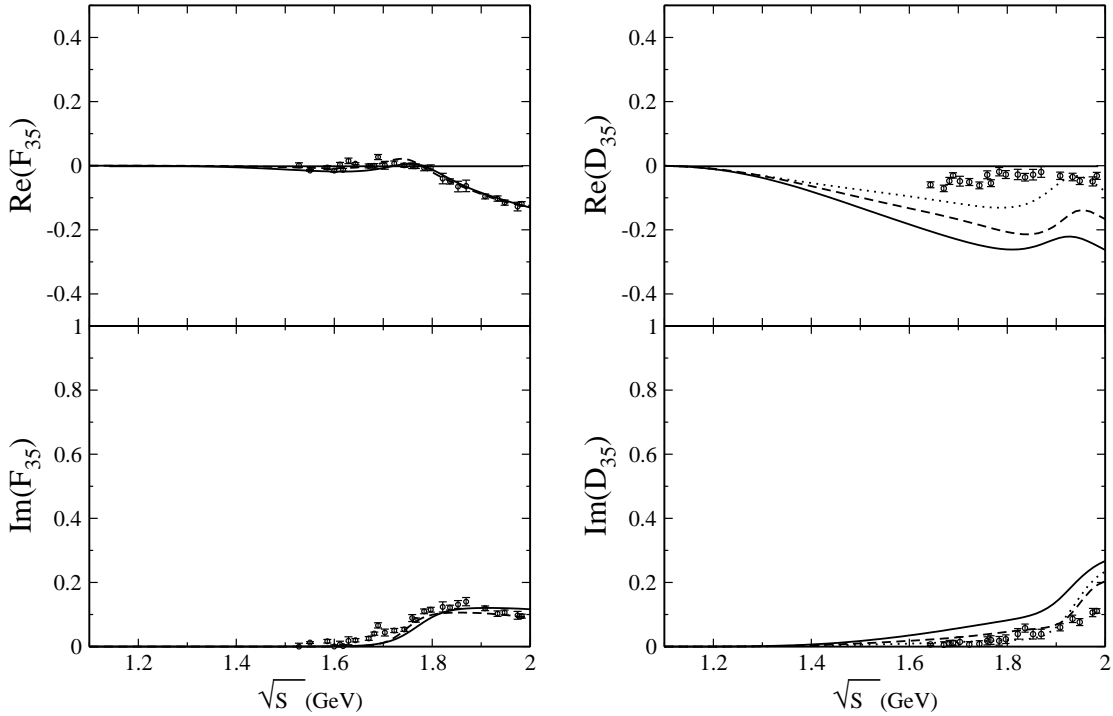


FIG. 2: The elastic $\pi N \rightarrow \pi N$ scattering amplitudes for the spin- $\frac{5}{2}$ partial waves. The solid (dashed) line corresponds to calculation C-p- $\pi + (\frac{5}{2})$ (P-p- $\pi + (\frac{5}{2})$). The dotted line in the right figure is the result for reduced nucleon cutoff (see text). The data are taken from [25].

the $2\pi N$ and inelasticity data runs into 2 mb at 1.67 GeV. This flux can be absorbed by neither ηN , $K\Lambda$, $K\Sigma$, ωN channels, see Fig. 4. Thus we conclude that either the πN and $2\pi N$ data are inconsistent with each other or other open channels (as $3\pi N$) must be taken into account. To overcome this problem and to describe the πN and $2\pi N$ data in the D_{15} partial wave the original $2\pi N$ data error bars [22] were weighted by a factor 3. The same procedure was also used by Vrana et al. [5] and Cutkosky et al. [26] to fit the inelastic data.

In both conventional and Pascalutsa coupling calculations the total inelasticities in the D_{15} wave almost coincide with the partial wave cross sections and therefore are not shown in Fig. 3 (left top). A good description of the inelasticity in the D_{15} wave was achieved and the extracted resonance parameters are also in agreement with other findings (see next section).

F₁₅. The $F_{15}(1680)$ and $F_{15}(2000)$ resonances are identified in this partial wave. The inclusion of the second resonance significantly improves the description of the πN and $2\pi N$ experimental data in the higher-energy region. Some evidence for this state was also found in earlier works [4, 23]. A visible inconsistency between the inelastic VPI data and the $2\pi N$ cross section from [22] above 1.7 GeV can be seen in Fig. 3 (left bottom). The three data points at 1.7, 1.725, and 1.755 GeV have, therefore, not been included in our calculations. Finally we achieve a reasonable description for both πN and $2\pi N$ data. The conventional and Pascalutsa coupling calculations give approximately the same results.

F₃₅. A single resonance state $F_{35}(1905)$ was taken into account. Some other models find an additional lower-lying resonance with a mass of about 1.75 GeV [4, 5, 23, 27]. However, we already find a good description of the elastic πN amplitudes and the $2\pi N$ cross sections by only including the single $F_{35}(1905)$ state. The inclusion of a second state with somewhat lower mass leads to a worse description of the πN and $2\pi N$ data due to the strong interference between the nearby states. The two $2\pi N$ data points at 1.87 and 1.91 GeV, which are apparently above the total inelasticity have not been included into calculations.

The total inelasticity in the F_{35} partial wave almost coincides with the calculated $2\pi N$ cross section and is not shown in Fig. 3. Note, that the $2\pi N$ data at 1.7 GeV are slightly below the total inelasticity from [25]. This could indicate that other inelastic channels give additional contributions to this partial wave.

There are also difficulties in the description of the $2\pi N$ low-energy tails of the D_{15} and F_{15} partial waves below 1.6 GeV, where the calculated cross sections are slightly below the $2\pi N$ data. The discrepancy leads to a significant rise in $\chi^2_{\pi 2\pi}$ (cf. Table I). The same behavior has been found in our previous calculations for the D_{13} partial waves

$L_{2I,2S}$	mass	Γ_{tot}	$R_{\pi N}$	$R_{2\pi N}$	$R_{\eta N}$	$R_{K\Lambda}$	$R_{K\Sigma}$	$R_{\omega N}$
$D_{15}(1675)$	1665	144	40.2	59.1(−)	0.6(−)	0.0(+)	−0.04 ^a	—
	1662	138	41.2	58.4(+)	0.4(−)	0.0(−)	0.02 ^a	—
$F_{15}(1680)$	1674	120	68.5	31.5(−)	0.1(+)	0.0(+)	0.07 ^a	—
	1669	122	65.8	34.2(+)	0.0(−)	0.0(+)	0.13 ^a	—
$F_{15}(2000)$	1981	361	9.0	84.0(+)	4.3(−)	0.5 ^b (−)	0.4(−)	2.2
	1986	488	9.5	88.2(−)	0.3(−)	0.1(+)	0.2(−)	1.7
$F_{35}(1905)$	1859	400	11.3	88.7(+)	—	—	0.7 ^b (+)	—
	1830	457	10.3	89.7(−)	—	—	0.0(+)	—

TABLE II: Properties of the spin- $\frac{5}{2}$ resonances considered in the present calculation. The first line corresponds to calculation C-p- $\pi + (\frac{5}{2})$ and the second to P-p- $\pi + (\frac{5}{2})$. Masses and total widths Γ_{tot} are given in MeV. The decay ratios R are shown in percent of the total width. ^a: The coupling is presented since the resonance is below threshold. ^b: Decay ratio in 0.1%.

[8]. There, it has been suggested that the problem might be caused by the description of the $2\pi N$ channel in terms of an effective ζN state. Indeed, the findings of [4, 5] show strong $\pi\Delta$ decay ratios in all three D_{15} , F_{15} , and F_{35} partial waves. The description of the $2\pi N$ channel in terms of the ρN and $\pi\Delta$ channels may change the situation when taking into account the ρN and $\pi\Delta$ phase spaces and corresponding spectral functions. Upcoming calculations will address this question.

D₃₅. A single $D_{35}(1930)$ resonance is taken into account. However, there is no clear resonance structure in the πN data for this partial wave. The data [25] also show a total inelasticity at the 2 mb level whereas the $2\pi N$ channel was found to be negligible [22]. It has been suggested [22] that this channel could have an important inelastic $3\pi N$ contribution. Since the measured $2\pi N$ cross section is zero we have used the inelastic πN data with enlarged error bars instead of the $2\pi N$ data to pin down the $2\pi N D_{35}$ contributions. Even in this case we have found difficulties in the description of the D_{35} partial wave. The πN channel turns to be strongly influenced by the u -channel nucleon and resonance contributions which give significant contributions to the real part of D_{35} . As can be seen in Fig.2 the conventional and Pascalutsa coupling calculations cannot give even a rough description of the experimental data [25]. The situation can be improved by either using the reduced nucleon cutoff Λ_N or by neglecting the nucleon u -channel contribution in the interaction kernel. The latter approximation has been used in the coupled-channel approach of Lutz et al. [28]. To illustrate this point we have carried out an additional fit for the reduced cutoff $\Lambda_N=0.91$ taking only the πN and $2\pi N$ data into account. The calculated χ^2 are $\chi^2_{\pi\pi}=3.63$ and $\chi^2_{\pi 2\pi}=7.87$ where the D_{35} data are also taken into account in (13) (note, that all values in Table I are calculated by neglecting these datapoints). The results for the D_{35} partial wave are shown in Fig. 2 by the dotted line. In all calculations for D_{35} presented in Fig. 2 the $D_{35}(1930)$ mass was found to be of about 2050 MeV. One sees that the calculations with a reduced nucleon cutoff lead to a better description of the D_{35} data giving, however, a worse description of other πN partial wave data. Note, that a reduction of the nucleon cutoff is required for a successful description of the lower-spin photoproduction multipoles [8, 9] which also leads to a worsening in χ^2 for the πN channel. Here we leave the problem of description of the D_{35} partial wave for future study when the photoproduction data will be also included thus allowing more constrain for the background contributions.

Finally, we conclude that the main features of the considered spin- $\frac{5}{2}$ partial waves except D_{35} are well reproduced. From Figs. 1-3 one can see that there is no significant difference between the conventional (8) and the Pascalutsa (11) spin- $\frac{5}{2}$ couplings. The results for the lower-lying spin- $\frac{1}{2}$ and $-\frac{3}{2}$ partial waves are only slightly changed from our previous study [8] and we do not show them here.

V. EXTRACTED RESONANCE PARAMETERS

A. Spin- $\frac{5}{2}$ states

The extracted parameters of the spin- $\frac{5}{2}$ resonances are presented in Table II. We note that the total resonance widths calculated here do not necessarily coincide with the full widths at half maximum because of the energy dependence of the decay widths (4, 7) and the formfactors used [8]. We do not show here the parameters of the $D_{35}(1930)$ resonance because of problems in the $D_{35}(1930)$ partial wave (see the previous Section). Although a good description of the experimental data is achieved some differences in the extracted resonance parameters for the conventional and the

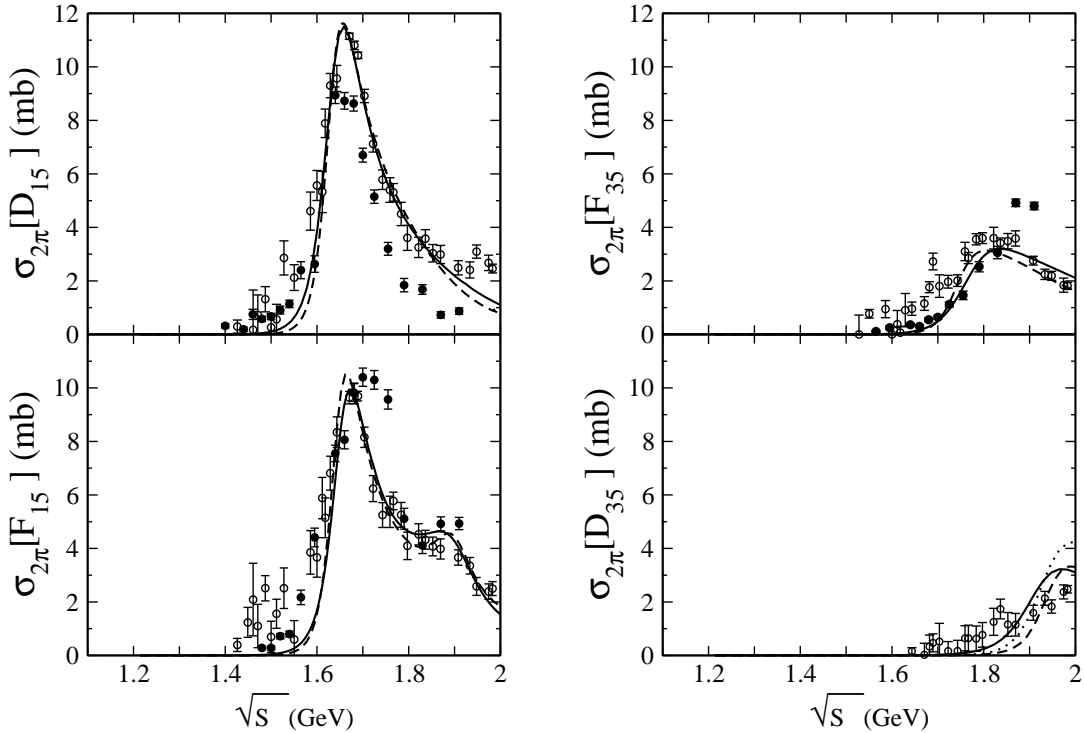


FIG. 3: The inelastic D_{15} , F_{15} , F_{35} , and D_{35} waves. The solid (dashed) line corresponds to calculation C-p- $\pi + (\frac{5}{2})$ (P-p- $\pi + (\frac{5}{2})$) for the $2\pi N$ channel. Open and filled circles represent the total inelasticity from the VPI group [25] and the $2\pi N$ data [22], respectively. The calculated inelasticities almost coincide with the calculated $2\pi N$ cross sections and are not shown here. Calculation with a reduced nucleon cutoff is shown by the dotted line.

Pascalutsa coupling calculations exist.

We obtain a little lower mass for the $D_{15}(1675)$ as compared to that obtained by Manley and Saleski [4] and Vrana et al. [5], but in agreement with other findings [29, 30]. The total width is found to be consistent with the results from [5, 23, 29]. In the ηN channel our calculations show a small ($\approx 0.6\%$) decay fraction which is somewhat higher than the value obtained by Batinić et al. : $0.1 \pm 0.1\%$ [30], whereas Vrana et al. give another bound: $\pm 1\%$. We conclude that both fits give approximately the same results for the resonance masses and branching ratios.

The properties of the $F_{15}(1680)$ state are found to be in good agreement with the values recommended by [1]. We find a somewhat smaller branching ratio in the ηN channel as compared to that of [30]. However, the obtained value $R_{\eta N} = 0.1\%$ is again in agreement with the findings of Vrana et al. [5]: $\pm 1\%$. The parameters of the second $F_{15}(2000)$ resonance differ strongly in various analyses: Manley and Saleski give 490 ± 310 MeV for the total decay width while other studies [3, 23] find it at the level of 95 – 170 MeV. Moreover, this state has not been identified in the investigations of [5, 30]. Although we find different results for Γ_{tot} in the two independent calculations, the branching ratios are close to each other. A small decay width of about 4.3% is found for the ηN channel (C-p- $\pi + (\frac{5}{2})$). However, since the $F_{15}(2000)$ resonance is found to be strongly inelastic with 84-88% of inelasticity absorbed by the $2\pi N$ channel, the more rich $2\pi N$ data above 1.8 GeV (cf. Fig. 3) are needed for a reliable determination of the properties of this state.

The parameters of the $F_{35}(1905)$ state are in good agreement with [1]. Both fits give approximately the same result for the decay branching ratios.

Although the extracted resonance masses and total widths can differ for the conventional and the Pascalutsa descriptions we find that the branching ratios are almost identical in both cases. Apart from the πN and $2\pi N$ final states we find no other significant contributions to the D_{15} , F_{15} , and F_{35} waves. All considered resonances have a negligible decay ratio to the ηN , $K\Lambda$, $K\Sigma$, and ωN channels. The only exception is the $F_{15}(2000)$ resonance where a small decay width to ηN has been found for the conventional coupling calculations. Note that there are also small contributions to the ωN channel. We corroborate the results of the previous study [8] where the main contribution to this channel is found to come from the P_{11} and P_{13} partial waves.

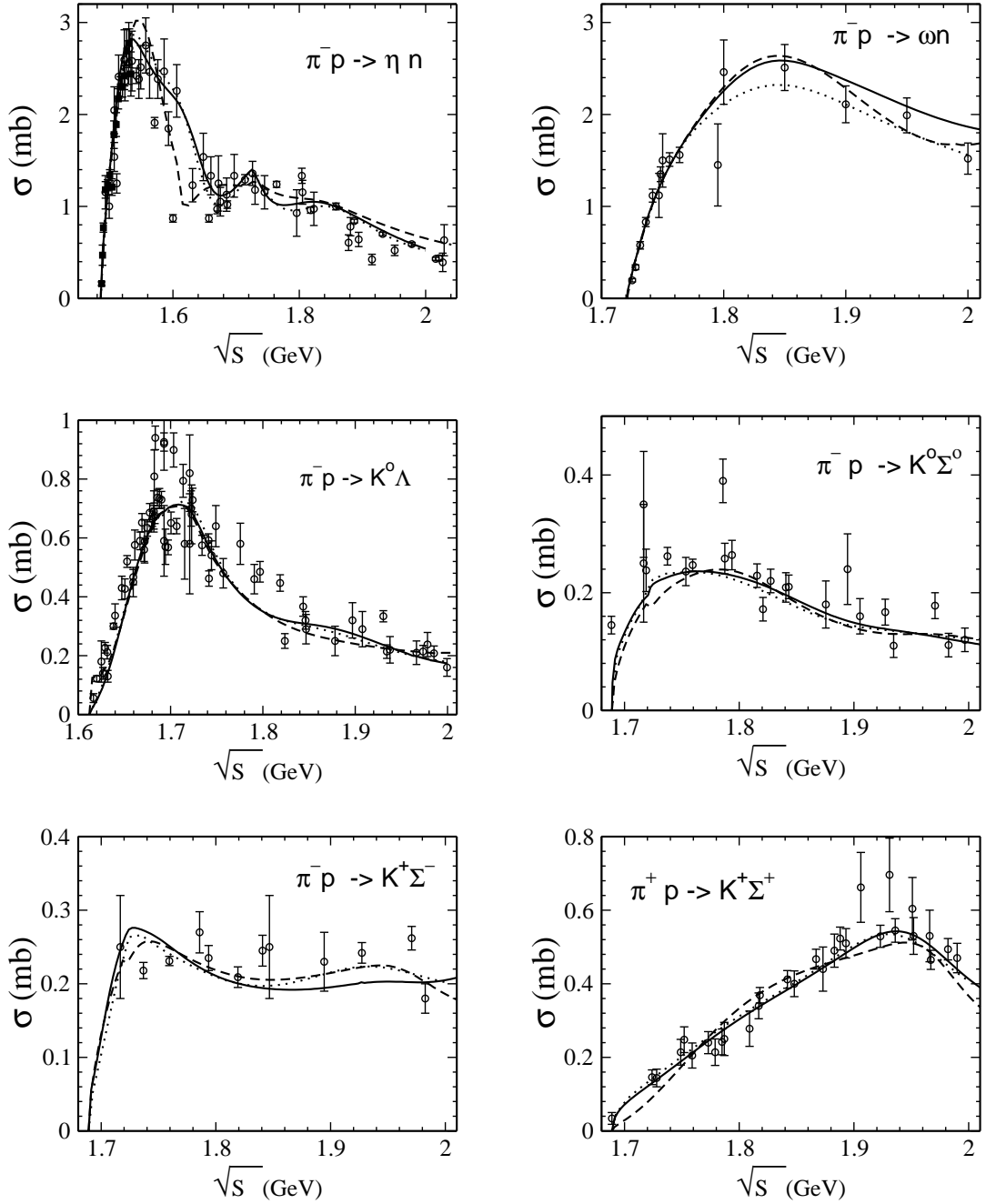


FIG. 4: The total cross sections for the inelastic reactions. The solid (dashed) line corresponds to calculation C-p- $\pi + (\frac{5}{2})$ (P-p- $\pi + (\frac{5}{2})$) result. The dotted line shows our previous results C-p- $\pi +$ [8]. For data references see [6].

B. The lower spin states

In Fig. 4 the results for the ηN , $K\Lambda$, $K\Sigma$, and ωN total cross sections are shown. We find a good description of all available experimental data including the angle-differential observables in these final states. The coupled channel effects show up in a kink structure of the total ηN , $K^0\Sigma^0$, and $K^+\Sigma^-$ cross sections at 1.72 GeV reflecting the opening of the ωN channel. Both calculations give the same results for the total cross sections in all channels except the $\pi^- p \rightarrow \eta n$ reaction [8]. For comparison our previous best hadronic fit result C-p- $\pi +$ from [8] is shown by the dotted line. The calculated cross sections almost coincide with our previous results in the conventional coupling

$L_{2I,2S}$	mass	Γ_{tot}	$R_{\pi N}$	$R_{2\pi N}$	$R_{K\Sigma}$
$S_{31}(1620)$	1614	169	36.9	63.1(−)	0.91 ^a
	1612	175	36.0	64.0(−)	0.94 ^a
	1630	177	42.5	57.5(+)	0.47 ^a
	1630	177	43.4	56.6(+)	0.48 ^a
$S_{31}(1900)^P$	1987	236	30.1	69.8(−)	0.1(−)
	1984	237	30.4	69.5(−)	0.1(−)
$P_{31}(1750)$	1752	630	1.9	97.4(+)	0.7(+)
	1752	632	2.3	97.2(+)	0.6(+)
	1978	664	19.8	78.9(+)	1.3(−)
	1975	676	19.5	79.4(+)	1.1(−)
$P_{33}(1232)$	1230	104	100.0	0.001(+)	—
	1231	101	100.0	0.002 ^b (+)	—
	1230	94	100.0	0.0(+)	—
	1230	94	100.0	0.000 ^b (+)	—
$P_{33}(1600)$	1652	244	14.3	85.7(+)	0.16 ^a
	1652	273	13.7	86.3(+)	0.22 ^a
	1660	371	13.7	86.3(+)	0.30 ^a
	1656	350	13.2	86.8(+)	0.28 ^a
$P_{33}(1920)$	2057	514	12.5	82.7(−)	4.7(−)
	2057	527	15.5	79.5(−)	5.0(−)
	2060	437	8.1	86.5(−)	5.4(−)
	2056	435	9.1	86.8(−)	4.1(−)
$D_{33}(1700)$	1677	652	13.8	86.2(+)	2.11 ^a
	1680	591	13.6	86.4(+)	2.09 ^a
	1673	671	14.6	85.4(+)	3.70 ^a
	1674	678	14.6	85.4(+)	3.68 ^a

TABLE III: Properties of $I = \frac{3}{2}$ resonances considered in the present calculation. Masses and total widths Γ_{tot} are given in MeV, the decay ratios R in percent of the total width. In brackets, the sign of the coupling is given (all πN couplings are chosen to be positive). ^{*P*}: Only found in the Pascalutsa calculations. ^{*a*}: The coupling is given since the resonance is below threshold. ^{*b*}: Decay ratio in 0.1%. 1st line: C-p- $\pi^+(\frac{5}{2})$, 2nd line: C-p- π^+ , 3rd P-p- $\pi^+(\frac{5}{2})$, 4th line: P-p- π^+ .

calculations. A visible difference between our previous and the new results is seen in the ωN total cross sections. Indeed, only a few datapoints are available above 1.8 GeV so that the ωN total cross section is not strongly constrained by the experimental data. This in turn leads to the different ωN resonance decay widths for the $D_{13}(1950)$ state as compared to our previous calculations [8].

The extracted lower spin resonance properties are hardly changed in comparison with the previous findings [8]. However, the inclusion of the spin- $\frac{5}{2}$ states leads to some modification of the isospin- $\frac{1}{2}$ baryon resonance parameters. We discuss these states only when apparent differences with earlier studies are found.

The results for isospin- $\frac{3}{2}(\frac{1}{2})$ resonance parameters are presented in Table III (IV). In Tables V and VI a comparison with the values given by the partial data group [1] and parameters from [4, 5] are shown. All resonance states investigated in our previous work [8] were included in the present calculations. We corroborate all the resonances identified in [8]. One sees that the inclusion of spin- $\frac{5}{2}$ resonances hardly affects the results for the isospin- $\frac{3}{2}$ resonance properties.

Some deviations in comparison with our previous studies are found for the isospin- $\frac{1}{2}$ resonances, see Table IV. We obtain a somewhat larger width for the Roper resonance $P_{11}(1440)$ in the new C-p- $\pi^+(\frac{5}{2})$ calculations. Indeed the properties of this state are found to be very sensitive to background contributions [8, 9]. The inclusion of the spin- $\frac{5}{2}$ states gives an additional lower-spin background which leads to the increase of the total width for the conventional spin- $\frac{5}{2}$ coupling calculation in comparison with that obtained in the previous study [8]. The branching ratios are found to be in agreement with the values recommended in [1].

The $P_{11}(1710)$ resonance has a three-star status and its properties are not completely established [1]. The parameters

$L_{2I,2S}$	mass	Γ_{tot}	$R_{\pi N}$	$R_{2\pi N}$	$R_{\eta N}$	$R_{K\Lambda}$	$R_{K\Sigma}$	$R_{\omega N}$
$S_{11}(1535)$	1540	156	35.7	11.2(+)	53.1(+)	0.02 ^a	-2.54 ^a	—
	1542	148	37.7	11.5(+)	50.8(+)	0.02 ^a	0.27 ^a	—
	1548	125	34.4	0.4(−)	65.2(+)	-4.46 ^a	0.43 ^a	—
	1545	117	36.6	0.9(−)	62.6(+)	-4.46 ^a	0.26 ^a	—
$S_{11}(1650)$	1676	161	65.4	19.6(+)	6.4(−)	8.6(−)	-0.53 ^a	—
	1671	158	65.1	22.7(+)	5.1(−)	7.1(−)	-0.54 ^a	—
	1703	294	68.0	14.3(−)	4.9(+)	12.8(−)	-0.36 ^a	—
	1699	276	68.2	14.7(−)	3.8(+)	13.3(−)	-0.50 ^a	—
$P_{11}(1440)$	1508	571	60.7	39.3(+)	3.51 ^a	3.43 ^a	-2.22 ^a	—
	1490	463	61.5	38.5(+)	3.27 ^a	3.43 ^a	-1.01 ^a	—
	1516	644	60.5	39.5(+)	3.17 ^a	1.97 ^a	3.67 ^a	—
	1515	639	60.6	39.4(+)	4.17 ^a	1.97 ^a	3.64 ^a	—
$P_{11}(1710)$	1753	534	2.3	30.7(+)	26.2(−)	0.1(+)	20.8(−)	19.9
	1770	430	2.0	42.7(+)	31.6(−)	0.9(+)	6.3(−)	16.4
	1704	380	7.8	27.8(−)	35.6(+)	26.6(−)	2.3(−)	—
	1701	348	8.5	25.7(−)	38.3(+)	26.3(−)	1.3(−)	—
$P_{13}(1720)$	1725	267	12.2	66.2(+)	2.1(−)	8.1(−)	10.6(−)	0.8
	1724	295	15.4	65.2(+)	1.2(+)	9.9(−)	7.5(−)	0.7
	1694	170	15.8	82.7(+)	0.1(+)	1.1(+)	0.4(+)	—
	1700	148	14.2	83.1(+)	0.0(+)	1.7(+)	1.0(+)	—
$P_{13}(1900)$	1962	700	24.7	52.8(−)	9.3(+)	3.5(−)	0.1(+)	9.6
	1962	683	19.1	58.2(−)	11.9(+)	1.9(−)	0.8(+)	8.1
	1948	792	23.5	51.7(−)	8.3(+)	0.8(+)	0.3(+)	15.5
	1963	694	15.7	58.2(−)	3.0(+)	0.1(+)	0.0(+)	22.9
$D_{13}(1520)$	1508	91	58.9	41.1(−)	1.4 ^b (+)	0.44 ^a	1.47 ^a	—
	1512	95	58.7	41.3(−)	3.1 ^b (+)	0.44 ^a	1.20 ^a	—
	1509	93	60.7	39.3(−)	1.5 ^b (+)	0.86 ^a	-3.32 ^a	—
	1509	91	60.1	39.9(−)	2.2 ^b (+)	0.86 ^a	-3.23 ^a	—
$D_{13}(1700)^P$	1743	67	0.8	31.5(+)	4.4(+)	4.3(−)	1.4(−)	57.6
	1745	55	1.6	43.4(+)	1.7(+)	6.7(−)	1.2(−)	45.3
$D_{13}(1950)$	1927	855	15.5	33.2(+)	0.4(−)	1.2(+)	2.6(+)	47.0
	1946	885	16.2	49.1(+)	2.2(−)	1.2(+)	1.9(+)	29.4
	1946	703	14.1	56.0(+)	0.0(+)	2.0(−)	0.8(+)	27.1
	1943	573	13.3	50.8(+)	0.0(−)	2.2(−)	0.7(+)	32.9

TABLE IV: Properties of $I = \frac{1}{2}$ resonances considered in the calculation. Notation is the same as in Table III.

of this state are also found to be strongly influenced by the lower spin off-shell contributions from the spin- $\frac{5}{2}$ resonances in the conventional coupling calculations. While the πN decay width remains almost unchanged, the additional background affects the inelastic channels and the fit moves the strength from $2\pi N$ and ηN to the $K\Sigma$ and ωN final states. This also leads to the decrease of the $\Lambda_{\frac{1}{2}}$ (see Table VII). The resulting $K\Sigma$ decay width turns out to be rather large: $R_{K\Sigma}=21\%$. We conclude that the properties of the $P_{11}(1710)$ state are rather sensitive to background contributions in the conventional coupling calculations. While the conventional couplings lead to different resonance properties in the P_{11} partial wave as compared to our previous study the resonance parameters in the Pascalutsa coupling calculations are only slightly changed. The $P_{11}(1710)$ resonance width $\Gamma_{tot}=534(430)$ MeV obtained in the conventional (Pascalutsa) coupling calculation is in agreement with the findings [4] (see Table VI) but smaller than the results from [5, 26, 31]. We also find the ηN ratio about 25-30%, close to the result of Batinić et al. [30].

There are two resonances ($P_{13}(1720)$ and $P_{13}(1900)$) included in the P_{13} wave. It is interesting to look at the results for the $P_{13}(1900)$ resonance in the Pascalutsa coupling calculations. Although the Pascalutsa spin- $\frac{5}{2}$ coupling does not have any lower-spin off-shell background and therefore does not directly affect the πN and $2\pi N$ lower-spin partial

$L_{2I,2S}$	mass	Γ_{tot}	$R_{\pi N}$	$R_{2\pi N}$	$R_{K\Sigma}$
$S_{31}(1620)$	1614	169	36.9	63	
	1620	150	25(5)	75(5)	
	1672(7)	154(37)	9(2)		
	1617(15)	143(42)	45(5)		
$S_{31}(1900)^P$	1987	236	30	70	0.1
	1900	200	20(10)		
	1920(24)	263(39)		41(4)	
	1802(87)	48(45)	33(10)		
$P_{31}(1750)$	1752	630	1.9	97.4	0.7
	1750	300	8(3)		
	1744(36)	300(120)	8(3)		
	1721(61)	70(50)	6(9)		
$P_{33}(1232)$	1230	104	100.0	0.001	
	1232	120	> 99	0	
	1231(1)	118(4)	100		
	1234(5)	112(18)	100(1)		
$P_{33}(1600)$	1652	244	14.3	86	
	1600	350	18(7)	82(8)	
	1706(10)	430(73)	12(2)		
	1687(44)	493(75)	28(5)		
$P_{33}(1920)$	2057	514	12.5	82.7	4.7
	1920	200	13(7)		
	2014(16)	152(55)	2(2)		
	1889(100)	123(53)	5(4)		
$D_{33}(1700)$	1677	652	14	86	
	1700	300	15(5)	85(5)	
	1762(44)	600(250)	14(6)		
	1732(23)	119(70)	5(1)		
$F_{35}(1905)$	1859	400	11	89	0.7 ^b
	1905	350	10(5)	90(5)	
	1881(18)	327(51)	12(3)		
	1873(77)	461(111)	9(1)		

TABLE V: Properties of $I = \frac{3}{2}$ resonances for the calculation C-p- π^+ ($\frac{5}{2}$) (1st line) in comparison with the values from [1] (2nd line), [4] (3rd line), and [5] (4th line). In brackets, the estimated errors are given. The mass and total width are given in MeV, the decay ratios in percent. ^b: The decay ratio is given in 0.1%. ^P: Calculation P-p- π^+ ($\frac{5}{2}$).

waves, the inclusion of the spin- $\frac{5}{2}$ resonances gives additional contributions to the ηN , $K\Lambda$, $K\Sigma$, and ωN channels. The fit has tried to compensate these changes giving also somewhat different values for the πN and $2\pi N$ decay widths as compared to our previous results. The same effect is seen in the properties of the $D_{13}(1700)$ resonance where noticeable changes in the $2\pi N$ and ωN channels are also observed (cf. Table IV). Note, that although the resonance mass of the $P_{13}(1900)$ is rather well fixed here, the inclusion of photoproduction data may change the situation [8, 9].

As in the case of the $P_{11}(1710)$ resonance, the properties of the $D_{13}(1950)$ state are also influenced by the spin- $\frac{5}{2}$ off-shell contributions in the conventional coupling calculations. The most striking difference between our previous and the new results for the $D_{13}(1950)$ state is found in the $2\pi N$ and ωN channels. Here the $2\pi N$ -flux is moved to the ωN channel. On the other hand, the investigations of photo-induced reactions [9] show that the D_{13} resonances play a minor role in ωN when the photoproduction data are included. We corroborate our previous findings that using only $\pi N \rightarrow \omega N$ is not sufficient for a reliable determination of the ωN strength in each partial wave.

Finally, we conclude that the inclusion of the spin- $\frac{5}{2}$ resonances leads to some modifications of the resonance parameters extracted in our previous study [8]. While the properties of the isospin- $\frac{3}{2}$ states are hardly changed,

$L_{2I,2S}$	mass	Γ_{tot}	$R_{\pi N}$	$R_{2\pi N}$	$R_{\eta N}$	$R_{K\Lambda}$	$R_{K\Sigma}$	$R_{\omega N}$
$S_{11}(1535)$	1540	156	36	11	53			
	1535	150	45(10)	6(5)	43(12)			
	1534(7)	151(27)	51(5)					
	1542(3)	112(19)	35(8)		51(5)			
$S_{11}(1650)$	1676	161	65	20	6	9		
	1650	150	72(17)	15(5)	6(3)	7(4)		
	1659(9)	173(12)	89(7)					
	1689(12)	202(40)	74(2)		6(1)			
$P_{11}(1440)$	1508	571	61	39				
	1440	350	65(5)	35(5)				
	1462(10)	391(34)	69(3)					
	1479(80)	490(120)	72(5)		0(1)			
$P_{11}(1710)$	1753	534	2	31	26	0.1	21	20
	1710	100	15(5)	65(25)				
	1717(28)	480(230)	9(4)					
	1699(65)	143(100)	27(13)		6(1)			
$P_{13}(1720)$	1725	267	12	66	2	8	11	1
	1720	150	15(5)	> 70	4	8(7)		
	1717 (31)	380(180)	13(5)		4	1		
	1716(112)	121(39)	5(5)		4(1)			
$P_{13}(1900)$	1962	700	25	52	9	4	0.1	10
	1900	500						
	1879(17)	498(78)	26(6)					
	NF							
$D_{13}(1520)$	1508	91	59	41	^{1^b}			
	1520	120	55(5)	45(5)				
	1524(4)	124(8)	59(3)					
	1518(3)	124(4)	63(2)		0(1)			
$D_{13}(1700)^P$	1743	67	1	32	4	4	1	58
	1700	100	10(5)	90(5)		< 3		
	1737(44)	250(220)	1(2)					
	1736(33)	175(133)	4(2)		0(1)			
$D_{13}(1950)$	1927	855	16	33	0.4	1	3	47
	2080							
	1804(55)	450(185)	23(3)					
	2003(18)	1070(858)	13(3)		0(2)			
$D_{15}(1675)$	1665	144	40	59	1	0		
	1675	150	45(5)	55(5)	0(1)	< 1		
	1676(2)	159(7)	47(2)					
	1685(4)	131(10)	35(1)		0(1)			
$F_{15}(1680)$	1674	120	69	32	0.1	0		
	1680	130(10)	65(5)	35(5)	0(1)			
	1684(4)	139(8)	70(3)					
	1679(3)	128(9)	69(2)		0(1)			
$F_{15}(2000)$	1981	361	9	84	4	6.8 ^b	0.4	2
	2000							
	1903(87)	490(310)	8(5)					
	NF							

TABLE VI: Comparison of $I = \frac{1}{2}$ resonance properties. Notation as in Table V.

	Λ_N [GeV]	$\Lambda_{\frac{1}{2}}$ [GeV]	$\Lambda_{\frac{3}{2}}$ [GeV]	$\Lambda_{\frac{5}{2}}$ [GeV]	Λ_t [GeV]
C-p- $\pi+(\frac{5}{2})$	1.16	2.79	1.03	1.16	0.71
C-p- $\pi+$	1.16	3.64	1.04	—	0.70
P-p- $\pi+(\frac{5}{2})$	1.17	4.30	1.02	0.95	1.82
P-p- $\pi+$	1.17	4.30	1.02	—	1.80

TABLE VII: Results for the formfactor cutoff values for the formfactors in comparison with the previous findings. The lower index denotes the intermediate particle, i.e. N : nucleon, $\frac{1}{2}$: spin- $\frac{1}{2}$ resonance, $\frac{3}{2}$: spin- $\frac{3}{2}$, $\frac{5}{2}$: spin- $\frac{5}{2}$ resonance, t : t -channel meson.

the parameters of the isospin- $\frac{1}{2}$ resonances differ in some specific cases from those extracted in [8]. The largest changes of the decay ratios can be observed in the $2\pi N$, ηN , $K\Sigma$, and ωN channels, see Table IV. As stressed in [8] photoproduction data are inevitable for a reliable fixing of the resonance parameters.

The cutoff values obtained in the different calculations are shown in Table VII. Except for $\Lambda_{\frac{1}{2}}$ in the conventional coupling calculations, the results for the cutoff parameters remain unchanged in comparison with the previous findings. The decrease in this cutoff is caused by the influence of the additional spin- $\frac{1}{2}$ background contributions from the newly incorporated spin- $\frac{5}{2}$ resonances. Indeed, as discussed above, the inclusion of these states gives strong contributions to the P_{11} partial wave which increases the $P_{11}(1440)$ and the $P_{11}(1710)$ total widths. This effect leads to the modification of the spin- $\frac{1}{2}$ cuff-off giving a somewhat lower value as compared to our previous results. The large difference in Λ_t between the conventional and the Pascalutsa coupling calculations is related to the need for a larger t -channel non-resonant background in case of the Pascalutsa coupling calculations (see discussion in [8]).

VI. SUMMARY AND OUTLOOK

We have performed a first investigation of the pion-induced reactions on the nucleon within the effective Lagrangian K -matrix approach which includes the higher spin- $\frac{5}{2}$ resonances. To investigate the influence of additional background from the spin- $\frac{3}{2}$ and - $\frac{5}{2}$ resonances calculations using the conventional and Pascalutsa higher-spin couplings have been carried out. A good description of the available experimental data has been achieved in all πN , $2\pi N$, ηN , $K\Lambda$, $K\Sigma$, and ωN final states within both frameworks giving however a somewhat worse χ^2 for the Pascalutsa coupling prescription. Apart from $2\pi N$ we find no significant contributions from other channels to the total πN inelasticities in the spin- $\frac{5}{2}$ waves. Nevertheless, the inclusion of the higher-spin states improves the χ^2 in almost all channels.

We have also found evidence for the $F_{15}(2000)$ resonance which is rated two-star by [1] and has not been included in the most recent resonance analysis by Vrana et al. [5]. The small πN decay ratio shows the necessity for more precise $2\pi N$ data to identify this state more reliably in the purely hadronic calculations. For most resonances the extracted parameters for the lower-spin states have only slightly changed in the new calculations compared to those obtained in our previous study [8]. However, for some resonances deviations from [8] for the pure hadronic fits are observed. This underlines the necessity of the inclusion of photoproduction data to fix the resonance couplings with certainty. The extracted cutoff parameters are also in general identical to those obtained in the previous study.

We are proceeding with the extension of our model by performing a combined analysis of pion- and photon-induced reactions taking into account spin- $\frac{5}{2}$ states. Moreover the decomposition of the $2\pi N$ channel into intermediate ρN , $\pi\Delta$ etc. states will be the subject of further investigations.

[1] K. Hagiwara et al., Phys. Rev. D **66**, 010001 (2002), <http://pdg.lbl.gov>.

[2] S. Capstick and W. Roberts, nucl-th/0008028.

[3] R.A. Arndt, I.I. Strakovsky, R.L. Workman, and M.M. Pavan, Phys. Rev. C **52**, 2120 (1995).

[4] D.M. Manley and E.M. Saleski, Phys. Rev. D **45**, 4002 (1992).

[5] T.P. Vrana, S.A. Dytman, and T.-S.H. Lee, Phys. Rept. **328**, 181 (2000).

[6] T. Feuster and U. Mosel, Phys. Rev. C **58**, 457 (1998).

[7] T. Feuster and U. Mosel, Phys. Rev. C **59**, 460 (1999).

[8] G. Penner and U. Mosel, Phys. Rev. C **66**, 055211 (2002).

[9] G. Penner and U. Mosel, Phys. Rev. C **66**, 055212 (2002).

[10] G. Penner, PhD thesis, Universität Gießen, 2002, available via <http://theorie.physik.uni-giessen.de>.

- [11] W. Rarita and Schwinger, Phys. Rev. **60**, 61 (1941).
- [12] M. Zétényi and Gy. Wolf, nucl-th/0103062.
- [13] J.C. David, C. Fayard, G.H. Lamot, and B. Saghai, Phys. Rev. C **53**, 2613 (1996).
- [14] B.S. Han, M. K. Cheoun, K.S. Kim, and I.-T. Cheon, Nucl. Phys. **A691**, 713 (2001).
- [15] A. I. Titov, T.-S. H. Lee, Phys. Rev. C **66**, 015204 (2002).
- [16] L.M. Nath, B. Etemadi, and J.D. Kimel, Phys. Rev. D **3**, 2153 (1971); L.M. Nath and B.K. Bhattacharyya, Z. Phys. **C5**, 9 (1980).
- [17] M. Benmerrouche, R.M. Davidson, and N.C. Mukhopadhyay, Phys. Rev. C **39**, 2339 (1989); R.M. Davidson, N.C. Mukhopadhyay, and R. Wittman, Phys. Rev. Lett. **56**, 804 (1986).
- [18] V. Pascalutsa, Phys. Rev. D **58**, 096002 (1998); V. Pascalutsa and R. Timmermans, Phys. Rev. C **60**, 042201 (1999).
- [19] V. Pascalutsa, Phys. Lett. **B503**, 85 (2001).
- [20] V. Pascalutsa and J.A. Tjon, Phys. Rev. C **61**, 054003 (2000).
- [21] A.D. Lahiff and I.R. Afman, Phys. Rev. C **60**, 024608 (1999).
- [22] D.M. Manley, R.A. Arndt, Y. Goradia, and V.L. Teplitz, Phys. Rev. D **30**, 904 (1984).
- [23] G. Höhler, F. Kaiser, R. Koch, and E. Pietarinen, *Handbook of Pion-Nucleon scattering*, Landolt-Börnstein, [Physics Data No. 12-1, (1979)]
- [24] C. Sauermann, B.L. Friman, and W. Nörenberg, Phys. Lett. **B341**, 261 (1995); C. Deutsch-Sauermann, B. Friman, and W. Nörenberg, *ibid*, **B409**, 51 (1997).
- [25] M.M. Pavan, R.A. Arndt, I.I. Strakovsky, and R.L. Workman, Phys. Scr. **T87**, 62 (2000); nucl-th/9807087, R.A. Arndt, I.I. Strakovsky, R.L. Workman, and M.M. Pavan, Phys. Rev. **C52**, 2120 (1995), updates available via: <http://gwdac.phys.gwu.edu/>.
- [26] R.E. Cutkosky and S. Wang, Phys. Rev. D **42**, 235 (1990).
- [27] R.L. Kelly and R.E. Cutkosky, Phys. Rev. D **20**, 2782 (1979).
- [28] M.F.M Lutz, Gy. Wolf, and B. Friman, Nucl. Phys. **A706**, 431 (2002).
- [29] R.E. Cutkosky, C.P. Forsyth, J.B. Babcock, R.L. Kelly, and R.E. Hendrick, Presented at 4th Int. Conf. on Baryon Resonances, Toronto, Canada, Jul 14-16, 1980. Published in Baryon 1980:19.
R.E. Cutkosky, C.P. Forsyth, R.E. Hendrick and R.L. Kelly, Phys. Rev. D **20**, 2839 (1979).
- [30] M. Batinić, I. Šlaus, A. Švarc, and B.M.K. Nefkens, Phys. Rev. **C51**, 2310 (1995), *Erratum* *ibid*, **C57**, 1004 (1998); nucl-th/9703023; M. Clajus and B.M.K. Nefkens, πN -Newsletter **7**, 76 (1992).
- [31] R.A. Arndt, I.I. Strakovsky, and R.L. Workman, Phys. Rev. **C53**, 430 (1996).